ELSEVIER

Canadian Association of Radiologists Journal 61 (2010) 201–205

CANADIAN ASSOCIATION OF RADIOLOGISTS JOURNAL

www.carjonline.org

Neuroradiology / Neuroradiologie

Magnetic Resonance Cisternographic Evaluation of Glossopharyngeal, Vagus, and Accessory Nerves

Hatice Gul Hatipoglu, MD*, Tugba Durakoglugil, Bulent Sakman, Enis Yuksel

Department of Radiology, Ankara Numune Education and Research Hospital, Ankara, Turkey

Abstract

Purpose: The individual visualization of the glossopharyngeal, vagus, and accessory nerves has been a troublesome issue. After the recent developments in the microsurgical field, the detailed knowledge of the relationship of these nerves and the tumour has gained importance. The purpose of this study is to compare the visibility of each of these nerves.
Methods: Thirty patients (M/F: 14/16; mean age 52.46 years) with complaints of vertigo, tinnitus, and hearing loss were examined with routine temporal magnetic resonance imaging (MRI) study. The imaging protocol consisted of 3-dimensional fast imaging with steady state acquisition in axial and sagittal oblique planes in addition to routine sequences. These images were transferred to a workstation and reformatted. Visibility of the nerves was evaluated by consensus of 2 radiologists who used an evaluation scale of 2 (excellently visible), 1 (partially visible), to 0 (not visible).
Results: In 26 patients, both sides were scanned; in 4 patients, only one side was scanned. A total of 168 nerves were investigated. The rates for visualization for each nerve were as follows: glossopharyngeal nerve, 100% and 100%; vagus nerve, 67.9% and 100%; and accessory nerve, 10.8% and 83.85% on axial and sagittal oblique 3-dimensional fast imaging with steady state acquisition, respectively.
Conclusions: Glossopharyngeal, vagus, and accessory nerve assessment improved when images were obtained in the sagittal oblique plane to the jugular foramen.

Résumé

Objet: La visualisation et l'individualisation des nerfs glosso-pharyngiens, vagues et spinaux ont longtemps posé problème. Devant les récentes avancées de la microchirurgie, il est devenu important de connaître et de décrire le trajet de ces nerfs ainsi que leur relation avec les processus tumoraux locaux. Le but de cette étude est d'évaluer et de comparer la visibilité de ces nerfs.
Méthodes: Trente patients (14 hommes et 16 femmes; âge moyen de 52,46 ans) atteints de vertige, d'acouphène et de perte auditive ont bénéficié d'une exploration de l'oreille et de la base du crâne en imagerie par résonance magnétique (IRM). Le protocole comportait en sus de l'exploration habituelle une séquence 3D FIESTA en acquisition axiale et sagittal oblique. Les données étaient ensuite transférées sur console de travail et reconstruites. La visibilité des nerfs a été évaluée après consensus d'une lecture faite par deux radiologues suivant l'échelle de visibilité suivante : 2 : excellente, 1 : partielle et 0 : nulle.
Résultats: En tout, 56 côtés de 30 patients ont été évalués. Un total de 168 nerfs a été examiné. Les taux de visibilité en séquence 3D FIESTA en acquisition axiale et sagittal oblique étaient respectivement de 100 et 100 % pour le nerf glosso-pharyngien, de 67.9 et 100 % pour le nerf vague et de 10.8 et 83.35 % pour le nerf spinal.
Conclusions: La visibilité et l'individualisation des nerfs glosso-pharyngiens, vagues et spinaux étaient meilleure en acquisition 3D FIESTA lorsqu'un plan sagittal oblique au foramen jugulaire était utilisé.

Key Words: Magnetic resonance imaging; Cisternography; Vagus nerve; Glossopharyngeal nerve; Accessory nerve

The detailed evaluation of posterior fossa tumours and the surrounding neurovascular structures has gained importance after new developments in microsurgical techniques. The visualization of the glossopharyngeal nerve (CN IX), vagus

* Address for correspondence: Hatice Gul Hatipoglu, MD, Maresal Fevzi Cakmak cad., 64/A, 06500 Besevler, Ankara, Turkey.
E-mail address: gulhatip@yahoo.com (H. G. Hatipoglu).

0846-5371/$ - see front matter © 2010 Canadian Association of Radiologists. All rights reserved.
doi:10.1016/j.carj.2009.10.004

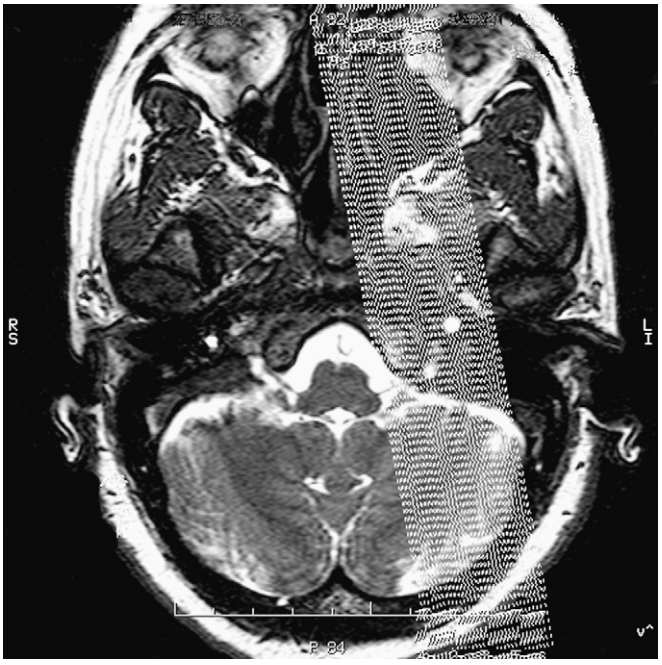

Figure 1. The 3-dimensional fast imaging with steady state acquisition sequence is obtained in the sagittal oblique plane in addition to the routine axial plane.

nerve (CN X), and accessory nerve (CN XI) in the cistern and jugular foramen level in relation to tumour have been a troublesome issue. Castillo and Mukherji [1] remarked about the potential role of combination of computed tomography (CT) and magnetic resonance imaging (MRI) in extensive evaluation of those nerves from the base of skull to the upper thorax. Nowadays, MRI has become the mainstream imaging modality [2]. MRI allows detailed evaluation of the nuclear origins and the normal course of the cranial nerves. CN IX, X, and XI are intimately located. They are regarded as a unit, the lower cranial nerve complex [1]. It is usually impossible to individually differentiate one from the other with routine MRI sequences. However, it is important to evaluate the nerves before surgery. The newer MRI sequences have potential for much better evaluation [3]. Contrast-enhanced 3-dimensional (3D) magnetization prepared rapid gradient echo (MP-RAGE) and 3D constructive interference steady state (CISS) sequences demonstrated the encasement of CN IX-XI in a case of adult pilocytic astrocytoma before surgery [4]. A broader study showed superiority of 3D sequences (CISS and MP-RAGE) when compared with 2-dimensional (2D) TSE T2-weighted sequences [5]. There few studies of MR (magnetic resonance) cisternography that used fast imaging with steady state acquisition (FIESTA) [6–8]. A selected group of posterior fossa tumour cases (12 schwannomas, 8 meningiomas, 3 epidermoid cysts) were successfully evaluated by 3D FIESTA sequence before surgery [6].

In this study, we sought to determine whether obtaining the images in the sagittal oblique plane could enhance the visualization of the glossopharyngeal, vagus, and accessory nerves compared with axial plane, which, in turn, could provide quick and reliable localization of the tumour-nerve intersurface at the jugular foramen–cistern level.

Materials and Methods

Thirty patients (M/F: 14 /16; mean age 52.46 years) with complaints of vertigo, tinnitus, and hearing loss were examined with a routine temporal MRI study. All examinations were performed on a 1.5 T whole-body MRI system (Excite; GE Medical Systems, Milwaukee, WI), with a 33 mT/m maximum gradient capacity. The imaging protocol consisted of 3D FIESTA (relaxation time [TR], 4.8 ms; echo time [TE], 1.4 ms; slice thickness, 0.5 mm; field of view [FOV], 18 × 18 cm; matrix, 352 × 192; number of excitations [NEX], 4) in the sagittal oblique plane in addition to routine sequences. The scans of the patients were in the sagittal oblique plane, which was more or less perpendicular to the nerves that pass through the jugular foramen (Figure 1). The imaging protocol of a temporal MRI study included the axially obtained 3D FIESTA. The images were transferred to an Advantage Workstation 4.0 (GE Medical Systems) and reformatted. A routine temporal MRI study included axial T1 W, T2 W, 3D FIESTA, and postcontrast axial and coronal T1 W sequences. The contrast agent used was 0.2 mL/kg gadolinium. T2 W images were obtained with fast spin echo sequences. The parameters for routine imaging were as follows: T1 W (TR, 500 ms; TE, 15.7 ms; slice thickness, 3 mm; interslice gap, 0.5 mm; FOV, 20 × 20 cm; matrix, 320 × 224; NEX, 3), T2 W (TR, 3000 ms; TE, 104.8 ms; slice thickness, 3 mm; interslice gap, 0.5 mm; FOV, 20 × 20 cm; matrix, 320 × 224; NEX, 3), 3D FIESTA (TR, 4.8 ms; TE, 1.4 ms; slice thickness, 0.5 mm; FOV, 18 × 18 cm; matrix, 352 × 192; NEX, 4). The consent forms were obtained according to the institutional guidelines. The visibility of 168 nerves was evaluated by consensus of 2 radiologists by using an evaluation scale of 2 (excellently visible), 1 (partially visible), to 0 (not visible). Cisternal parts of CN IX-XI were followed from the root exit zone from the brainstem to the cranial exit from jugular foramen on

Table 1
Visualization rates of CN IX, CN X, and CN XI on axial and sagittal oblique 3D FIESTA

	CN IX			CN X			CN XI		
Visualization rate	2	1	0	2	1	0	2	1	0
Axial 3D FIESTA, %	94.6	5.4	0	27.1	40.8	32.1	1.7	9.1	89.2
Sagittal oblique 3D FIESTA, %	100	0	0	100	0	0	80.3	3.55	16.15

CN IX = glossopharyngeal nerve; CN X = vagus nerve; CN XI = accessory nerve; 3D FIESTA = 3-dimensional fast imaging with steady state acquisition.

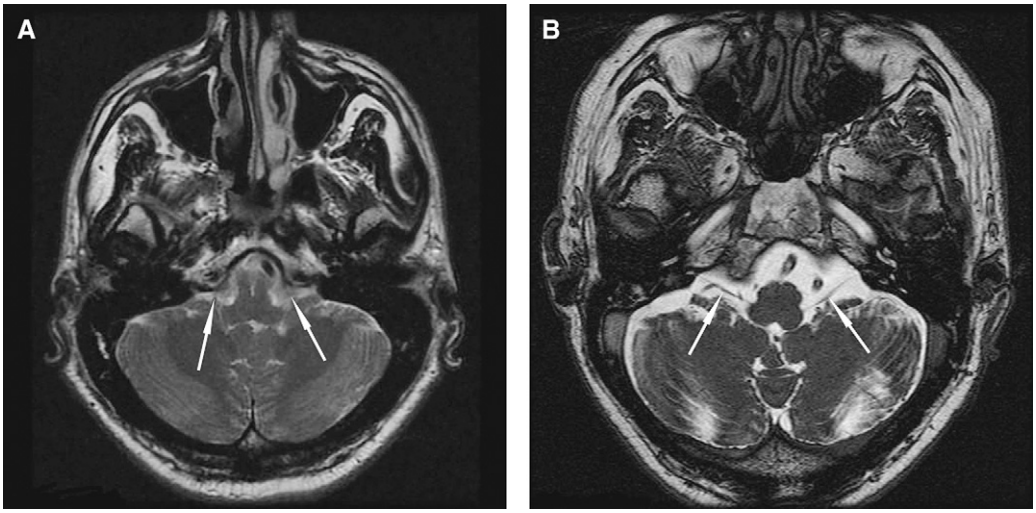

Figure 2. (A) Axial T2-weighted image is insufficient to demonstrate glossopharyngeal, vagus, and accessory nerves (arrows); the glossopharyngeal nerve is the easiest to identify on axial 3-dimensional fast imaging with steady state acquisition sequence (arrows). (B) It might be challenging for vagus and accessory nerves.

reformatted images. When the whole length of each nerve was visualized, it was considered ''excellently visible,'' and, if only some parts were visualized, then it was considered ''partially visible.'' Statistical analyses were performed with the SPSS 11.5 software program (SPSS Inc., Chicago, IL). Parametrical statistical methods were used for determining the visibility of cranial nerves in different MRI sequences.

Results

In our study, in all, 56 sides of 30 patients (in 26 patients, both sides were scanned; in 4 patients, only 1 side was scanned) were evaluated by axial fast spin echo (FSE) T2-weighted, axial and sagittal oblique 3D FIESTA sequences. In 4 patients, only 1 side was scanned in the sagittal oblique plane. A total of 168 nerves were investigated. Visualization rates of these cranial nerves (partially and completely visualized together) on axial and sagittal oblique 3D FIESTA sequences were as follows: glossopharyngeal nerve, 100% and 100%; vagus nerve, 67.9% and 100%; and spinal accessory nerve, 10.8% and 83.85%, respectively. Results are shown in detail in Table 1. We didn't visualize the nerves individually on FSE T2-weighted images in any of the cases.

Discussion

In the past, invasive methods, such as pneumoencephalography and high-resolution tomodensitometry, were performed with air and iodinized contrast agents to show the cranial nerves [8,9]. Today, MRI is preferred because it is noninvasive. There is no radiation exposure risk and has multiplanar imaging capability. Three-dimensional sequences are capable of showing structures that are smaller than 1 mm. MR cisternography is a new technique that was

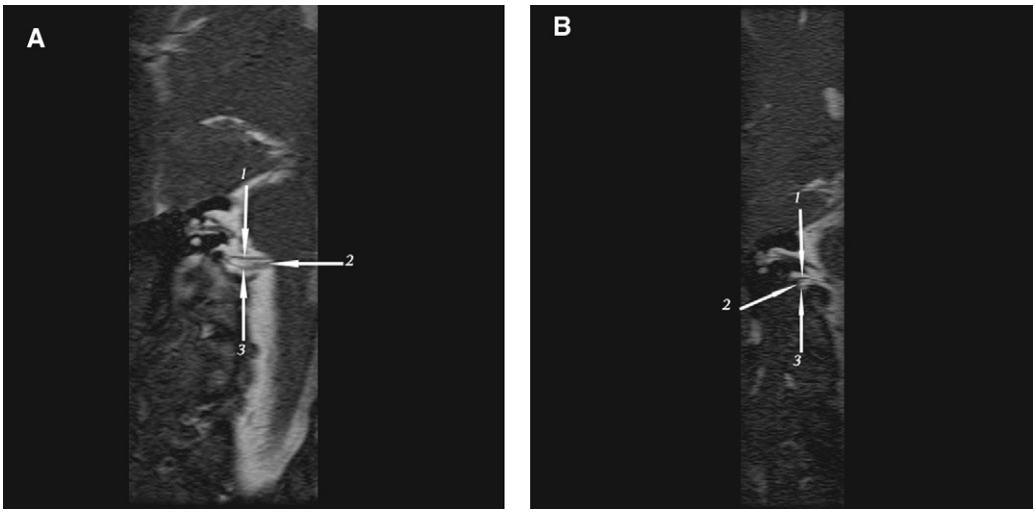

Figure 3. It is possible to visualize the whole length of the glossopharyngeal (1), vagus (2) and accessory (3) nerves in the cisternal (A) and foraminal (B) levels on consecutive images on 3-dimensional fast imaging with steady state acquisition sequence, which was obtained in the sagittal oblique plane and reformatted.

developed following improvements in 3D imaging; it is more effective than other sequences in demonstrating the neural structures and vessels in the cerebrospinal fluid. Visualizing the connection between tumoural lesions and neighbouring neurovascular structures before posterior fossa surgery affects the success of the procedure. The steady-state free precession (SSFP) technique is widely used for ultrafast cardiac or abdominal imaging. These are gradient echo sequences and their relaxation time (TR) is shorter than the tissue's T1 and T2 time. Transverse and longitudinal magnetization are never zero; they are in steady state. In these sequences, all of the signals accumulate because of the balance of gradients in all 3 dimensions. Accordingly, images with a high signal-to-noise ratio are achieved. Cerebrospinal fluid, blood, and fat have long T2 and T1 TR values so that they have high-signal intensity. Because of the fast imaging, movement and flow artifacts occur less often compared with other 3D sequences. Blurring artifacts occur less, because the MR signal is always achieved in a coherent state. Magnetic susceptibility artifacts occur with lower frequency because of the very short time of echo (TE) and wide band thickness [8,10]. The most frequently used SSFP sequences are balanced fast field echo (bFFE), balance turbo field echo (bTFE), true fast imaging with steady state precession (FISP), and FIESTA. As we mentioned earlier, there are only a few studies in the literature about MR cisternography with 3D FIESTA sequence. [6–8]. As far as we know, this is the first study that compared the axial and sagittal oblique plane 3D FIESTA obtained MR cisternography views in detailed evaluation of lower nerve complex from their nuclei in the medulla oblongata to their exit from the crania.

The jugular foramen contains the lower cranial nerve complex. The glossopharyngeal nerve enters into the most superior, anterior, and medial aspects of the endocranial opening of the jugular foramen [11]. Rubinstein et al [11] called the recess that the nerve enters ''glossopharyngeal meatus,'' which is inferior to the internal auditory canal and believed that it was a portion of the cochlear aqueduct. The vagus and accessory nerves could not be separated and visualized on CT images. At the entrance of the jugular foramen, these nerves are separated by only a few millimeters [11,12]. They are usually anterior to the jugular spine and, thereafter, travel anterior and medial to the jugular vein. The jugular foramen is divided into 2 at the endocranial opening, the anteromedial pars nervosa, which consists of the glossopharyngeal nerve and inferior petrosal sinus, and the posterolateral pars venosa, which contains the jugular vein, vagus, and accessory nerves. But as a different opinion according to Rubinstein, pars nervosa contains all 3 nerves [11]. In a study conducted by Ryan et al [13], accessory nerves originated from the spinal cord, with no distinct contribution from the medulla in 11 of 12 cases. In 1 case, a small connection was seen between vagus and the spinal accessory nerves within the jugular foramen [13]. Daniels et al [14,15] were the first to correlate the cryomicrotomic sections and axial T1-weighted gradient recalled echo images of the jugular foramen. They proved the superiority of gradient echo to the spin echo T1-weighted sequence. They also demonstrated that sagittal images were more useful than coronal or axial planes in the cadaver study.

Seitz et al [5] evaluated the visibility of the IXth-XIth cranial nerves in 30 healthy volunteers by using 2D T2-weighted, 3D CISS, and 3D MP-RAGE. As a result of the intersection gap and partial volume effects, the visualization on 2D T2-weighted sequence was limited. Although 3D sequences were much better, not all segments of the neural structures were visualized. In another study, 100% of the lower nerve complex as a unit were visible to some extent on a 3D FIESTA sequence as opposed to 67% on an FSE T2-weighted sequence [8]. In a study conducted by Okumuro et al [7], 66 nerves of 11 subjects were evaluated by 3D FIESTA. In all cases, CN IX and CN X were identified to some extent. The total visualization rate for CN XI was 91% [7].

In our study, axial FSE T2-weighted images were insufficient to individually visualize the glossopharyngeal, vagus, and spinal accessory nerves because of the intersection gap, partial volume effects, and cerebrospinal fluid flow artifact (Figure 2). When we looked at the reformatted axially obtained 3D FIESTA images, 5.4% of glossopharyngeal nerves were partially visualized. Only 27.1% of vagus and 1.7% of accessory nerves were visualized in whole segment. On reformatted 3D FIESTA, images that were obtained in the sagittal oblique plane, the whole-segment visualization rates dramatically improved to 100% for glossopharyngeal and vagus nerves and 80.3% for accessory nerve (Figure 3).

Conclusions

The MR cisternography images that were obtained in the sagittal oblique plane and reformatted would enable the assessment of glossopharyngeal, vagus, and accessory nerves individually. This would result in the detailed evaluation of the nerves in relation to tumour before resection with newly developed microsurgical techniques. Therefore, obtaining the images in the sagittal oblique plane should be considered in centers with an experienced team in skull base surgery instead of the axially obtained 3D sequences, which have become routine in most of the institutions.

References

[1] Castillo M, Mukherji SK. Magnetic resonance imaging of cranial nerves IX, X, XI, and XI. Top Magn Reson Imaging 1996;8:180–6.
[2] Larson III TC, Aulino JM, Laine FJ. Imaging of the glossopharyngeal, vagus, and accessory nerves. Semin Ultrasound CT MR 2002;23:238–55.
[3] Laine FJ, Underhill T. Imaging of the lower cranial nerves. Magn Reson Imaging Clin N Am 2002;10:433–49.
[4] Yousry I, Muacevic A, Olteanu-Nerbe V, et al. Exophytic pilocytic astrocytoma of the brain stem in an adult with encasement of the caudal cranial nerve complex (IX-XI): presurgical anatomical neuroimaging using MRI. Eur Radiol 2004;14:1169–73.

[5] Seitz J, Held P, Frund R, et al. Visualization of the IXth to XIth cranial nerves using 3-dimensional constructive interference in steady state, 3-dimensional magnetization-prepared rapid gradient echo and T2-weighted 2-dimensional turbo spin echo magnetic resonance imaging sequences. J Neuroimaging 2001;11:160−4.

[6] Mikami T, Minamida Y, Yamaki T, et al. Cranial nerve assessment in posterior fossa tumors with fast imaging employing steady-state acquisition (FIESTA). Neurosurg Rev 2005;28:261−6.

[7] Okumura Y, Suzuki M, Takemura A, et al. Visualization of the lower cranial nerves by 3D-FIESTA. Nippon Hoshasen Gijutsu Gakkai Zasshi 2005;61:291−7.

[8] Hatipoglu HG, Durakoglugil T, Ciliz D, et al. Comparison of FSE T2 W and 3D FIESTA sequences in the evaluation of posterior fossa cranial nerves with MR cisternography. Diagn Interv Radiol 2007;13:56−60.

[9] Seitz J, Held P, Strotzer M, et al. MR imaging of cranial nerve lesions using six different high resolution T1- and T2*-weighted 3D and 2D sequences. Acta Radiol 2002;43:349−53.

[10] Konez O. Manyetik rezonans görüntüleme: temel bilgiler [Magnetic resonance imaging: basic information]. Istanbul: Nobel; 1995. 53−78.

[11] Rubinstein D, Burton BS, Walker AL. The anatomy of the inferior petrosal sinus, glossopharyngeal nerve, vagus nerve, and accessory nerve in the jugular foramen. AJNR Am J Neuroradiol 1995;16: 185−94.

[12] Hatiboglu MT, Anıl A. Short report: structural variations in the jugular foramen of the human skull. J Anat 1992;180:191−6.

[13] Ryan S, Blyth P, Duggan N, et al. Is the cranial accessory nerve really a portion of the accessory nerve? Anatomy of the cranial nerves in the jugular foramen. Anat Sci Int 2007;82:1−7.

[14] Daniels DL, Schenck JF, Foster T, et al. Magnetic resonance imaging of the jugular foramen. AJNR Am J Neuroradiol 1985;6:699−703.

[15] Daniels DL, Czervionke LF, Pech P, et al. Gradient recalled echo MR imaging of the jugular foramen. AJNR Am J Neuroradiol 1988;9: 675−8.